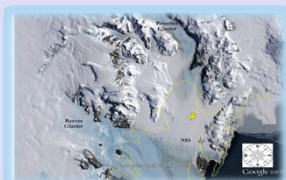


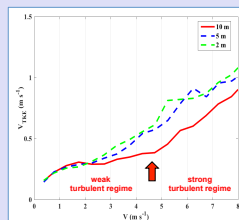
L. Mortarini<sup>1</sup>, D. Cava<sup>1</sup>, U. Giostra<sup>2</sup>, D. Anfossi<sup>1</sup><sup>1</sup> National Research Council, Institute of Atmospheric Sciences and Climate, Italy<sup>2</sup> Department of Pure and Applied Sciences (DiSPeA), Università degli Studi di Urbino "Carlo Bo", Urbino, Italy

**EXPERIMENTAL DATA.** In this work we analysed the impact of different submeso motions on the flow characteristics through the analysis of wind ( $u, v, w$ ) and temperature ( $T$ ) data collected above an Antarctic Ice Sheet during an austral summer. The site is prevalently interested by low winds blowing along valley axis and by persistent conditions of stable thermal stratification. Turbulence measurements were performed at three levels (2, 5, and 10 m) above the surface using symmetric 3-axis ultrasonic anemometers at a frequency of 20.8 Hz.



**Figure 1:** Satellite image of Victoria Land in West Antarctica. The star indicates the position of the micrometeorological tower located in the middle of a flat snowy homogeneous area on the Nansen Ice Sheet (NIS).

**Figure 2:** Relationship between the wind speed ( $V$ ) and the bin-averaged turbulence strength ( $V_{TKE} = [(1/2)(u'^2 + v'^2 + w'^2)]^{1/2}$ ) at the three measurement levels. The red arrow marks the transition between the weak and strong turbulent regimes at the highest measurement level, similar to the Hockey-stick transition (HOST) observed in Sun et al. (2012). This transition is not evident at the lowest levels because of the ground influence that increase the level of turbulence mixing.



### Gravity Waves triggered by sharp flow variations

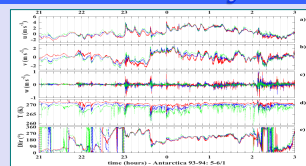


**Figure 7:** Time series collected on 5th January 1994 at 10 m (red lines), 5 m (blue lines) and 2 m (green lines).

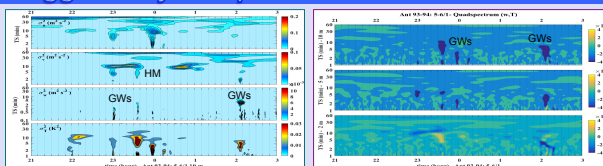


**Figure 8:** Time-frequency distribution of wavelet energy of wind components and temperature collected at 10 m (left) and quadrature of  $w$  and  $T$  at the different measurement levels (right), relative to the data set shown in Figure 7.

Another triggering mechanism for GWs generation are sharp variations of the wind direction often associated to strong temperature changes as shown in Figures 7 and 9. Figures 8 and 10 highlight GWs characterised by a period of about 10 minutes that persist just few cycles coincident to the sharp flow variations observed in Figures 7 and 9. The wavelet quadrspectrum clearly show a GWs activation at the highest level and its attenuation close to the ground.

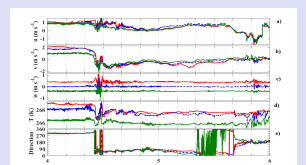
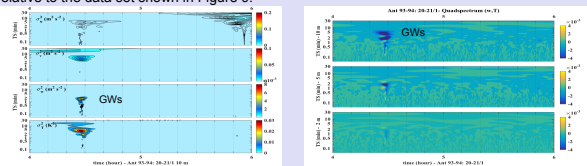


**Figure 9:** Time series collected on 20th January 1994 at 10 m (red lines), 4.5 m (blue lines) and 2 m (green lines).

**Figure 10:** Time-frequency distribution of wavelet energy of wind components and temperature collected at 10 m (left) and quadrature of  $w$  and  $T$  at the different measurement levels (right), relative to the data set shown in Figure 9.



#### References:

- Anfossi D, Oetti D, Degrazia G, Goulart A. 2005. An analysis of sonic anemometer observations in low wind speed conditions. *Boundary-Layer Meteorol.* **114**: 179 – 203.
- Cava D, Giostra U, Katul G. 2015. Characteristics of Gravity Waves over an Antarctic Ice Sheet during an Austral Summer. *Atmosphere* **6**: 1271-1289.
- Cava, D., Mortarini, L., Giostra U., Richardson, R., Anfossi, D. 2017. A wavelet analysis of low wind speed submeso motions in a nocturnal, boundary layer. *Quarterly Journal of Royal Meteorological Society.* **143**: 661 – 669.
- Mortarini L., Stefanelli M., Degrazia G., Roberti D., Trini Castelli S., Anfossi D. 2016. Characterization of Wind Meandering in Low-Wind-Speed Conditions, *Boundary Layer Meteorol.* **161**: 165 – 182.
- Sun J., Mahrt L., Banta R., Pichugina Y. 2012. Turbulence Regimes and Turbulence Intermittency in the Stable Boundary Layer during CASES-99. *Journal of the Atmos. Sci.* **69**: 338-351.

### Conclusions

In this work two different mechanisms for gravity waves activation have been investigated: gravity waves triggered by horizontal meandering or by sharp variation in the flow. Gravity waves triggered by horizontal meandering are often superimposed with a lower time scale, but with an activation period agreeing with the horizontal meandering period. Gravity waves triggered by sudden flow variation exhibit a period of about 10 minutes. In both cases gravity waves persist only few cycles and tend to be attenuated closer to the ground surface producing burst of turbulent mixing. The obtained results highlight the strong impact of non-stationary submeso motions on the structure of the intermittent turbulent flow during conditions of significant atmospheric stratification and weak winds.

**INTRODUCTION.** In a stable boundary layer (SBL) the flow is characterized by the complex interactions between the static stability of the air and non-turbulent processes that govern the mechanical generation of turbulence. Submeso motions can take a variety of forms including gravity waves, horizontal meandering modes, density currents, drainage flows. They can complicate the turbulence behaviour in the SBL and can modulate the turbulent fluxes through the production of intermittent mixing events related to localized flow acceleration.

### Horizontal Meandering and Gravity Waves

An important fraction of submeso motions is represented by horizontal meandering modes (HM), particularly when the large-scale flow is weak. For the analysis two different methodologies have been used: the first, specifically implemented for identifying meandering motions, based on the evaluation of Eulerian auto-correlation functions (EAFs) (Anfossi et al., 2005; Mortarini et al., 2016); and the second based on a Morlet continuous wavelet transform. Such combined approach enables a clear identification of periods interested by HM motions and the determination of their characteristic time scales (Cava et al., 2017).

The combined analyses highlight the prevalent occurrence of HM during nocturnal hours (between 16:00 and 06:00).

The wavelet analysis shows the frequent superimposition of meandering and intermittent gravity waves (GWs) characterised by different time scales. In Figures 3,4,5 the GWs are periodically triggered by HM that probably generates dynamical instabilities (i.e. shear or thermal instabilities). These GWs persist only few cycles and tend to be attenuated closer to the ground surface producing intermittent turbulence mixing.

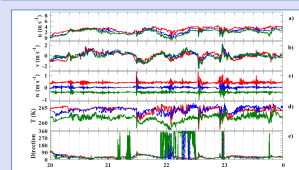


**Figure 3:** Time series collected on 25th November 1993 at 10 m (red lines), 5 m (blue lines) and 2 m (green lines).

**Figure 4:** Time-frequency distribution of wavelet energy of wind components and temperature collected at 10 m, relative to the data set shown in Figure 3.

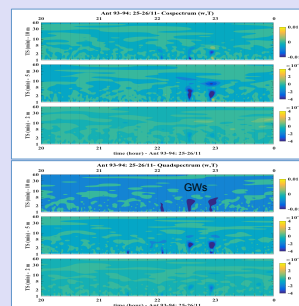
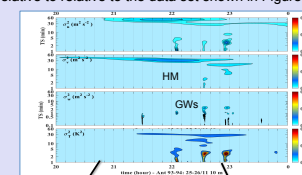


**Figure 5:** Time-frequency distribution of cospectrum (top) and quadrature (bottom) of  $w$  and  $T$  at the different measurement levels, relative to the data set shown in Figure 3.

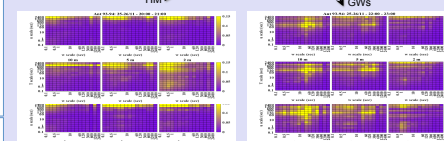


**Figure 6:** Standard deviation of  $w'u'$  (top),  $w'T'$  (middle),  $w'^2u'$  (bottom) MR decomposed time series for each combination of the scales and normalised by the standard deviation of the corresponding total flux time series relative to data at 20:00-21:00 (HM regime - left) and at 22:00-23:00 (GWs regime - right).



The selected periods are further analysed by using the multi-resolution (MR) decomposition useful to assess the amount of energy and flux variability due to the same scale eddies, or due to the joint interaction of eddy fluctuations of different scales. Figure 6 highlights the different energy and flux distribution in case of HM and GWs regimes (left and right, respectively): in the first regime the region of high variability is localised above the diagonal region, indicating that HM is responsible for local changes of shear that are subsequently responsible for turbulence generation; in the GWs regime the variability is mainly localized on the GWs scales.